Available online at www.sciencedirect.com
SCIENCE DIRECT
Remote Sensing of Environment 100 (2006) 388 – 406
Remote Sensing of Environment
www.elsevier.com/locate/rse

Integration of radar and Landsat-derived foliage projected cover for woody regrowth mapping, Queensland, Australia

Richard M. Lucas [a,*], Natasha Cronin [b], Mahta Moghaddam [c], Alex Lee [d], John Armston [b], Peter Bunting [a], Christian Witte [e]

[a] *Institute of Geography and Earth Sciences, The University of Wales, Aberystwyth, Penglais Campus, Aberystwyth, Ceredigion, SY23 3DB, United Kingdom*
[b] *Climate Impacts and Natural Resource Systems, Queensland Department of Natural Resources and Mines, Natural, Resource Sciences, 80 Meiers Road, Indooroopilly, Queensland, 4068, Australia*
[c] *Department of Electrical Engineering and Computer Science University of Michigan Ann Arbor, MI 48109, USA*
[d] *School of Resources, Environment and Society, the Australian National University, Canberra, ACT 0200, Australia*
[e] *Forest Ecosystem Research and Assessment, Queensland Department of Natural Resources and Mines, Natural, Resource Sciences Centre, 80 Meiers Road, Indooroopilly, Queensland, 4068, Australia*

Received 23 June 2005; received in revised form 15 September 2005; accepted 17 September 2005

Abstract

In Queensland, Australia, forest areas are discriminated from non-forest by applying a threshold (~12%) to Landsat-derived Foliage Projected Cover (FPC) layers (equating to ~20% canopy cover), which are produced routinely for the State. However, separation of woody regrowth following agricultural clearing cannot be undertaken with confidence, and is therefore not mapped routinely by State Agencies. Using fully polarimetric C-, L- and P-band NASA AIRSAR and Landsat FPC data for forests and agricultural land near Injune, central Queensland, we corroborate that woody regrowth dominated by Brigalow (*Acacia harpophylla*) cannot be discriminated using either FPC or indeed C-band data alone, because the rapid attainment of a canopy cover leads to similarities in both reflectance and backscatter with remnant forest. We also show that regrowth cannot be discriminated from non-forest areas using either L-band or P-band data alone. However, mapping can be achieved by thresholding and intersecting these layers, as regrowth is unique in supporting both a high FPC (>~12%) and C-band SAR backscatter (>~−18 dB at HV polarisation) and low L-band and P-band SAR backscatter (e.g. <=~14 dB at L-band HH polarisation). To provide a theoretical explanation, a wave scattering model based on that of Durden et al. [Durden, S.L., Van Zyl, J.J. & Zebker, H.A. (1989). Modelling and observation of radar polarization signature of forested areas. IEEE Trans. Geoscience and Remote Sensing, 27, 290–301.] was used to demonstrate that volume scattering from leaves and small branches in the upper canopy leads to increases in C-band backscattering (particularly HV polarisations) from regrowth, which increases proportionally with FPC. By contrast, low L-band and P-band backscatter occurs because of the lack of double bounce interactions at co-polarisations (particularly HH) and volume scattering at HV polarisation from the stems and branches, respectively, when their dimensions are smaller than the wavelength. Regrowth maps generated by applying simple thresholds to both FPC and AIRSAR L-band data showed a very close correspondence with those mapped using same-date 2.5 m Hymap data and an average 73.7% overlap with those mapped through time-series comparison of Landsat-derived land cover classifications. Regrowth mapped using Landsat-derived FPC from 1995 and JER-1 SAR data from 1994–1995 also corresponded with areas identified within the time-series classification and true colour stereo photographs for the same period. The integration of Landsat FPC and L-band SAR data is therefore expected to facilitate regrowth mapping across Queensland and other regions of Australia, particularly as Japan's Advanced Land Observing System (ALOS) Phase Arrayed L-band SAR (PALSAR), to be launched in 2006, will observe at both L-band HH and HV polarisations.

Keywords: Remote sensing; Synthetic aperture radar; Landsat; Regrowth mapping; Land cover change; Biomass; Queensland; Australia

* Corresponding author. Tel.: +44 1970 622612; fax: +44 1970 622659.
E-mail addresses: rml@aber.ac.uk (R.M. Lucas), Natasha.Cronin@nrm.qld.gov.au (N. Cronin), Mmoghad@eecs.umich.edu (M. Moghaddam), Alex.Lee@anu.edu.au (A. Lee), John.Armston@nrm.qld.gov.au (J. Armston), Christian.Witte@dnr.qld.gov.au (C. Witte).

0034-4257/$ - see front matter © 2005 Published by Elsevier Inc.
doi:10.1016/j.rse.2005.09.020

1. Introduction

Since European settlement, over half of Queensland's forests and woodlands (herein referred to as just forest) have been progressively cleared for agricultural development (Smith et al., 1994) and, despite recognition of the problems associated with their clearance, deforestation rates accelerated in the 1990s, with over 1 million ha cleared during the period 1999–2001. Much of the clearance in Queensland occurred in the more productive native forest ecosystems and particularly within the Brigalow Belt, a biogeographic region of south central Queensland, where over 52%, 57% and 59% of the statewide total occurred in 1991–1995, 1995–1997 and 1997–1999, respectively (Statewide Land Cover and Trees Study; SLATS, 1999). Such clearance has been documented from 1988 through land cover change detection based on Landsat-5 Thematic Mapper (TM) and Landsat-7 Enhanced TM (ETM+) data and has resulted in extensive losses of carbon, as indicated by Australia's National Greenhouse Gas Inventories (NGGI) for the State (AGO, 2002; AGO, 2005), increased levels of salinity (ACF, 2002), depletion of biodiversity (Fairfax & Fensham, 2000; NLWRA, 2002) and extinction of species (Environment Australia, 2001).

Across large areas of the State, extensive regrowth of woody vegetation is also evident, with the extent and rate of growth dependent largely upon prior land management practices and climatic variability (Fairfax & Fensham, 2000). One reason for the occurrence of woody regrowth in recent years is that extensive areas of forest were cleared in the year prior to proclamation of the Queensland Vegetation Management Act 1999 (15th September 2000) (SLATS, 2003). However, in many of the areas, pastoral land use has not been maintained and extensive areas of woody regrowth have inevitably started to appear. The species composition of the regrowth is often linked to that of the original forest prior to clearance and in the Brigalow Belt, large tracts are dominated by Brigalow (*Acacia harpophylla;* Henry et al., 2002; SLATS, 2003).

The mapping of this regrowth, both in cleared areas but also in forested areas subject to thickening (Burrows et al., 2000; Burrows et al., 2002; Henry et al., 2002), is critical for assessing greenhouse gas emissions and biodiversity values. Regrowth represents the primary mechanism by which forests can restore carbon, biological diversity and also function lost during clearance of the remnant vegetation. Forests in the early stages of growth represent a sink for carbon that is potentially enhanced by increased CO_2 levels in the atmosphere (Bond & Midgeley, 2000). Clearance of regrowth areas also leads to losses of carbon, which are lower than if remnant forests are cleared. For example, Henry et al. (2002) noted that of the 425,000 ha year^{-1} cleared in Queensland between 1997 and 1999, 138,000 ha^{-1} was estimated to be due to clearing of non-remnant or regrowth of a lower biomass than that associated typically with forests. Hence, improved knowledge of regrowth extent and both biomass and biomass increment can lead to better estimates of carbon emissions (e.g., for accounting of national greenhouse gas emissions). In terms of vegetation and land management, knowledge of regrowth extent and state is indicative of pasture degradation and can assist assessments of long-term agricultural productivity. Knowledge of the capacity of regrowth forests to recover biological diversity also assists conservation of habitats and their flora and fauna (Fairfax & Fensham, 2000). The provision of maps showing the age class distribution of forest areas is also now required following the introduction of legislation that requires permits for clearing stands older than 15 years (Environment Australia, 2001).

Despite the importance of regrowth, its mapping represents a significant challenge (Fensham et al., 1998; NGGI, 1997) and no reliable technique currently exists. There are several reasons for this.

- Regrowth dominated by species such as Brigalow often attains a cover equivalent to or exceeding that of the more intact and mature (herein referred to as remnant) forests, where forests are defined as vegetation greater than 2 m in height with a minimum crown cover of 20% (National Forest Inventory, 2003). A crown cover of 20% is suggested as being equivalent to a Foliage Projected Cover (FPC) of 12% (SLATS, 2003). FPC is defined as the horizontal percentage cover of photosynthetic foliage of all strata and provides a more appropriate estimate of the photosynthetic potential of the landscape due to the low density foliage of Australian vegetation (Specht & Specht, 1999). Herein, FPC refers to the overstorey component only, which includes trees and shrubs above 2 m (Kuhnell et al., 1998). The relationship between crown cover and FPC will vary according to the Leaf Area Index (LAI), leaf angle and foliage clumping of a forest stand, and is the subject of a forthcoming paper by SLATS.
- Queensland legislation defines non-remnant vegetation, which consists largely of regrowth, as having less than 70% of the height or 50% of the cover of the dominant stratum relative to "normal" height and cover. However, the height differences cannot currently be retrieved at a regional level using remote sensing data and hence statewide mapping is reliant on cover, as estimated from Landsat sensor data. For this reason, areas of mature and regrowth woody vegetation are not separated in maps of woody vegetation produced by the Queensland Department of Natural Resources and Mines (QDNRM) (SLATS, 2003).
- The spectral reflectance of regenerating vegetation is sensitive primarily to cover and is therefore often similar to that of remnant forest, especially during the later stages of growth. Reflectance is also influenced by the presence or otherwise of photosynthetic herbaceous cover, particularly following wet periods.
- Mapping regrowth through comparison of classifications generated from historical land cover data is limited because Landsat sensor data are available only from 1986 onwards, and from 1988 in most cases. Areas cleared or regrowth establishing prior to this date cannot be easily mapped because of the lack of appropriate datasets. Although historical aerial photography is available, regional 'wall-to-wall' mapping is impractical with these data, although sampling represents an alternative (Fensham et al., 1998).

- The mapping of regrowth by relating structural development to the progression of Landsat sensor reflectance data or derived products (e.g., FPC, NDVI, endmember fractions) over time is also problematic as intra- and inter-annual variations between dates may be associated with phenological variation and uncertainties resulting from spatial and temporal differences in atmospheric composition and bidirectional reflectance.

Although maps of the extent of regrowth are important, knowledge of regrowth structure and biomass is also needed, particularly for assessments of habitat, vegetation management practices, and carbon accumulation and turnover, but is similarly difficult to obtain from optical remote sensing data. Using Landsat data, for example, only a two-dimensional overview of vegetation is provided and hence differences or changes in the vertical structure of woody vegetation, which might be indicative of age and hence biomass, are difficult to assess from measures such as FPC alone. Relationships have been established between FPC and basal area, which are often used for approximating biomass (Back et al., 1999; Burrows et al., 2000; Burrows et al., 2002), but these tend to be less robust for Brigalow-type regrowth because of the disproportionately high FPC typical of these forests.

Recognising the difficulty in characterising and mapping woody regrowth using both single date and multi-temporal Landsat sensor data, we present a new method for mapping that integrates Landsat-derived FPC with low frequency L-band or P-band Synthetic Aperture Radar (SAR) data acquired by airborne and/or spaceborne sensors. We provide a theoretical basis for the detection of woody regrowth by parameterising a wave scattering model, based on that of Durden et al. (1989), with structural and biomass data obtained for regrowth forests through ground survey and published allometric data. Using this model, we simulate the backscattering coefficient (σ°) for different height and density configurations and at selected frequencies and polarisations to establish why mapping of Brigalow-type regrowth can be achieved using a combination of FPC and low frequency SAR. A particular advantage of the mapping method is that it can be applied across large areas using data from spaceborne optical sensors and the forthcoming Advanced Land Observing Satellite (ALOS) Phase Arrayed L-band SAR (PALSAR; Rosenqvist et al., 2003).

2. Characteristics of woody regrowth

In the Brigalow Belt, many areas of woody regrowth are dominated by *Acacia* species, particularly Brigalow (Scanlan, 1991), which is of the mallee classification; McDonald et al., 1990) and was once widespread across the region, occupying an area of 107,000 km^2. This species is associated with a range of forest classes, including low open woodland, open woodland, woodland and open forest (NFI, 1998). Brigalow with Eucalyptus (e.g., *Eucalyptus populnea*) emergents up to 20–25 m in height and a shrub layer ~2–6 m in height and consisting of either Sandalwood Box (*Eremophila mitchelli*) or Wilga (*Geijeira parviflora*) is commonplace. On more fertile soils, Brigalow is also associated with Belah (*Casuarina cristata*) along with a variety of softwood species, such as Narrow leaved bottle trees (*Brachychiton rupestris*).

By 1995, approximately 85% of land supporting Brigalow had been cleared, with much of the clearing and thinning occurring as long ago as 50 years (Fairfax & Fensham, 2000). For this reason, many established Brigalow stands resemble low open woodlands rather than the open forests typical during pre-European settlement. Where disturbed, Brigalow commonly forms large thickets known as 'Brigalow scrub' Mature scrub, which can be as high as 10–15 m if left relatively undisturbed, typically contains a number of layers formed through the natural differentiated growth of the species, dead trees, young trees, tall and small shrubs, herbs and grasses (EPA, 2000).

When clearing and subsequent regeneration occurs, the structure and species composition is often altered (Fairfax & Fensham, 2000). In areas of low open woodland, for example, where Brigalow has been cleared and then burnt, rapid suckering from the root butt of this species is commonplace (Johnson, 1964; Scanlan, 1991; Fig. 1a). If stock is then left to graze on the emerging suckers, the decapitation of plant parts leads to coppicing which reinvigorates and even accelerates

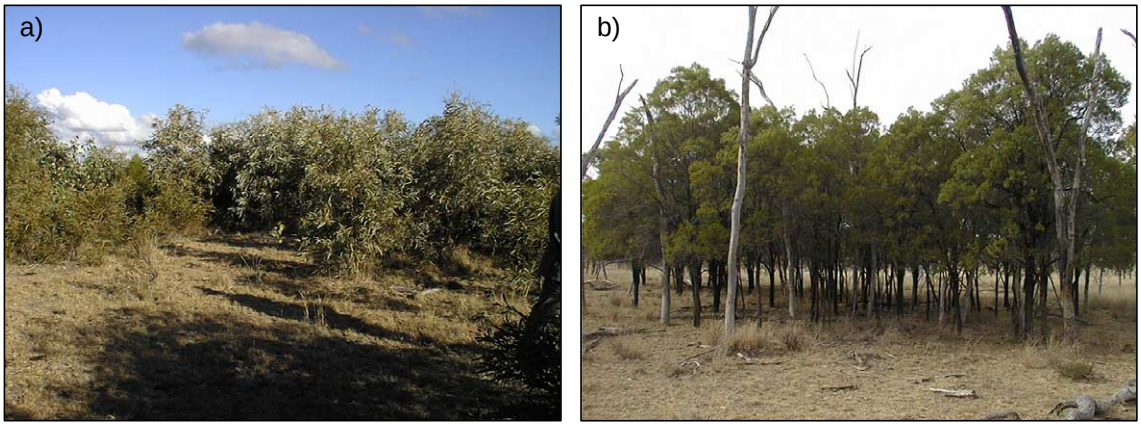

Fig. 1. (a) Brigalow regrowth with large leaf biomass and a large number of multiple stems (<3–5 cm) diameter and (b) clusters of Sandalwood Box (*Eremophila mitchelli*) supporting similar leaf biomass but fewer stems of greater diameter.

growth in some species (Burrows et al., 1990). This process also tends to encourage numerous slender trunks to regenerate from the root stock, thereby drastically altering the root to shoot relationship of the plants and increasing density (Ceulemans et al., 1996). This ability to coppice confers a degree of resilience to natural and anthropogenic disturbance and hence coppiced stands become extensive following the formation and subsequent neglect or abandonment of agricultural land. The greater number of stems per hectare and the faster growth rate (compared to individual seedlings; Burrows et al., 1990) of sprouts from the already established root system also leads to the rapid development of a canopy and the formation of relatively homogeneous stands, particularly as most other plant growth is excluded. The densities of stems (suckers) can approach 25,000 per hectare (QLD DPI, 1984; Scanlan, 1991) but despite the formation of a dense canopy, the basal area of these stands remains low (Kuhnell et al., 1998). When these trees become taller (e.g. $>\sim 5$ m), the number of stems reduces to one or two bases at ground level, and the dimensions (e.g. diameter) of each are greater. This later stage of regeneration, commonly referred to as whipstick brigalow, is typically of lower density (2000–5000 stems ha^{-1}; Johnson, 1964). These regrowth stands differ from those dominated by other (e.g., *Eucalyptus, Eremophila*) species where trees are often more widely spaced and support single or a few multiple stems of comparatively greater size (Fig. 1b).

3. Study site description

The study focused on a 37×60 km area of forest and agricultural land near Injune (Latitude $-25°32'$, Longitude $147°32'$), which is located in the Southern Brigalow Belt (Fig. 2). Approximately 75% of the area is occupied by leasehold properties whilst the remaining area encompasses several State Forests (Crown Land), including Attica, Koolbellup, Simpson and Hillside. Proximal townships include Tambo, Augathella, Mitchell and Injune whilst Roma is the nearest regional centre. Mean annual rainfall is approximately 635 mm $year^{-1}$, is variable with most recorded between December and February (summer) and the mean annual maximum temperatures for summer and winter are 27 °C and 11 °C, respectively (Bureau of Meteorology, 2004).

The natural vegetation of the region consists predominantly of low open woodland, open woodland, woodland and open forest (Galloway, 1974). The distribution of vegetation is determined largely by the geology, soil and topography/geomorphology (Neldner, 1984), with open Eucalyptus forest dominating the better sandy and clay soils and White Cypress Pine (*Callitris glaucophylla*) occurring on the poorer sandy soils. On the clay soils also, Brigalow is commonplace whilst within the open forests of the plateau, Iron barks (e.g., silver-leaved ironbark; *Eucalyptus melanaphloia*) are frequent.

The species composition, structure and biomass of the forests are determined by both natural and anthropogenic factors. Wildfires, although irregular, pass through the area and alteration of the species composition or dominance may occur, particularly as some species (e.g., *C. glaucophylla*) are less resistant to fire than others (Harris et al., 2003). Anthropogenic clearing (typically through chaining) has also been widespread and has occurred largely to facilitate establishment of cattle pasture. Partial clearance of vegetation has been commonplace in the pastoral areas and woody thickening has been observed (Burrows et al., 2000). Due to the complex nature of land use and management practices, the landscape consists of a mosaic of cleared fields and forest and woodland communities in various stages of degradation and/or regeneration (Lucas et al., 2004).

4. Materials and methods

4.1. Sampling design

The sampling design was undertaken in the knowledge that large scale (1:4000) aerial photography (herein referred to as

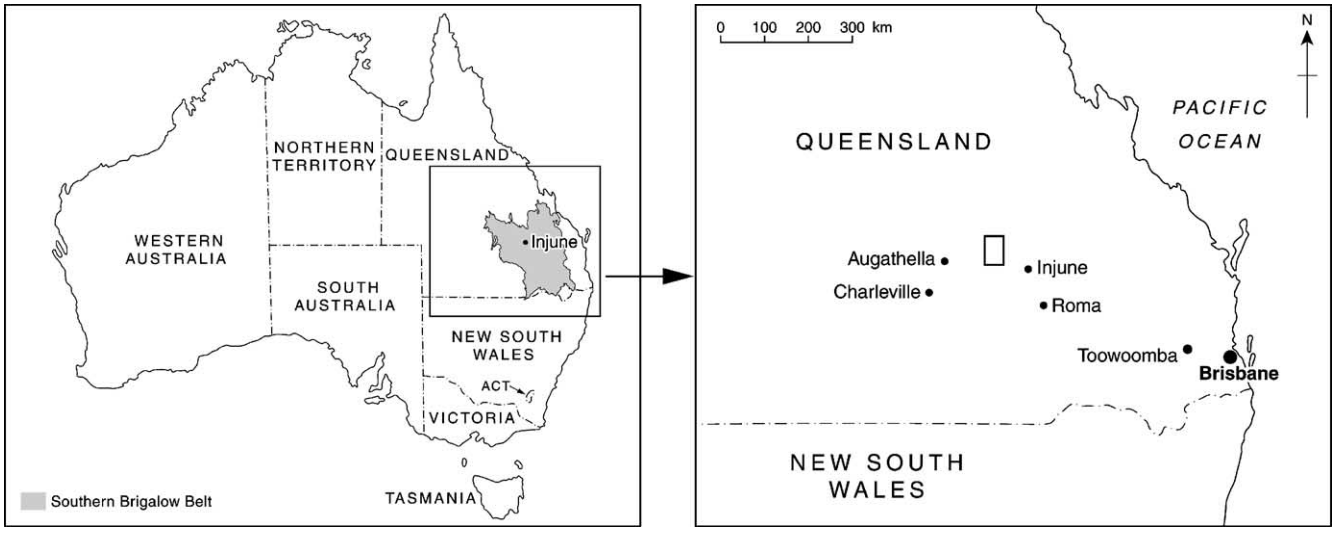

Fig. 2. The Injune study area.

LSP) was to be acquired over the 37 × 60 km study area. A systematic grid of 150 (10 columns numbered from east to west and 15 rows numbered from north to south starting from the north west corner) 800 × 800 m (64 ha) Primary Photo Plots (PPPs) was therefore established, with each PPP centre located 4 km apart in the north–south and east–west directions (Fig. 3). Within each PPP, a 150 × 500 m Primary Sampling Unit (PSU) was positioned to encompass the area of potential LSP overlap (Fig. 3). The scheme also divided each of the 150 PSUs into 30 Secondary Sampling Units (SSU), 50 × 50 m (0.25) in dimension and numbered progressively by row from top left (1) to bottom right (30). Based on this scheme, the equivalent of 4500 × 0.25 ha (i.e., 1125 ha) was sampled by the PSUs/SSUs, which collectively represented 0.46% of the 240,000 ha study area. A detailed overview of the scheme is provided by Lucas et al. (2004).

4.2. Remote sensing data acquisition: Aerial photography and SAR

For each of the 150 PPPs, and using pre-defined coordinates, 1:4000 LSP (in negative format) were acquired on the 11th July 2000 by QASCO Surveys Pty. Ltd. on behalf of the Queensland Department of Natural Resources and Mines (QDNRM) Landcare Centre. Photographs were taken using an RC20 large format photographic camera from late morning to mid afternoon. The effective swath width was 920 m with a 60% (50 ha) overlap corresponding to the approximate size of a PSU. For each photo principle point, GPS coordinates were recorded with a nominal precision of ±20 m. As 150 PPPs were sampled, 300 frames of photographs were obtained. Following delivery of the 150 hard copy stereo pairs, the main vegetation communities were differentiated and delineated manually within the PPP and specifically within the area of stereo overlap (equivalent to the PSU) by a trained photogrammetrist and described in terms of their species composition, height, cover and disturbance (Jones, 2000).

On 3rd September 2000, fully polarimetric C-band (5.6 cm or 5.3 GHz), L-band (23.9 cm, 1.25 GHz) and P-band (68 cm wavelength, 0.44 GHz frequency) band data were acquired by the NASA JPL AIRSAR (on board a DC-8) across the entire PSU grid, and also across an area extending ~20 km to the south. The POLSAR data were acquired in four parallel strips (S1–S4; length and width approximately 80 km and 12.5 km, respectively) in a "race track" path trajectory and from an altitude of ~8294 m. Interpretation of the LSP and ground survey established that extensive areas of woody regrowth were evident only in the west and to the south of the study area, and so only two of the four POLSAR strips were used for the analysis presented in this paper. The POLSAR images were synthesized from the 16-look compressed Stokes Matrix into HH, VV and HV polarisations (as well as total power, TP) to a pixel resolution in range and azimuth of 4.62 m. These data, in units of σ°, were slant-to-ground range corrected to a nominal resolution of 5 m (Van Zyl et al., 1987; Zebker et al., 1987). Geometric rectification to Universal Transverse Mercator (UTM) coordinates was achieved using ground control points (GCPs) established between each of the AIRSAR strips and Landsat ETM+ data of the study area acquired 2nd September 2000. These data had been georeferenced previously (to a spatial resolution of 25 m) using an independent set of GCPs and procedures standardised within the SLATS project (SLATS, 2003). Between 100 and 150 GCPs were established for each POLSAR strip, generating r.m.s. errors of <10 m after a third order polynomial nearest neighbour transformation was applied during the registration process. Comparison with LSP confirmed high registration accuracy. Following georeferencing, each ground range image was resampled to 10 m spatial resolution through pixel aggregation. Topographic correction was not applied as the terrain within the 37 × 60 study area was considered to be largely "flat", consisting of valley bottoms, plains or plateaux, or slightly undulating hills. As the influence of incidence angle on the retrieval of above ground biomass was a topic of interest (Lucas et al., 2005), no corrections were undertaken. Hyperspectral HyMap strips (~1.2 km swath width), consisting of 128 bands of visible to shortwave infrared data at 2.6 m spatial resolution, were also acquired in September 2000 for sections of PSU columns 1–4 and 8–9. These data were georeferenced using Inertial Navigation Systems (INS) and Global Positioning Systems (GPS).

4.3. Determination of FPC from Landsat sensor data

A stand scale allometric estimate of FPC is estimated routinely from Landsat TM and ETM+ data by SLATS based on empirical relationships established between FPC, basal area and reflectance data. For completeness, an overview of the method is summarised in this paper, although refer to Danaher et al. (2004) for further information.

SLATS obtained path-orientated Landsat-5 Thematic Mapper (TM) data through the Australian Centre for Remote Sensing (ACRES) for 1988, 1991, 1993, 1995 and 1997 and Landsat-7 Enhanced TM (ETM+) data for 2000. These data were acquired in the dry season (May–October) to maximise spectral contrast between perennial and herbaceous vegetation due to the senescence of annual grasses. The Landsat TM data were calibrated by replacing the on-board radiometric calibration with vicarious calibration based on a model of the lifetime response of the sensor (De Vries et al., 2004). Pre-flight coefficients were used to calibrate the Landsat-7 ETM+ data to radiance (NASA, 2004). All imagery was then corrected for bidirectional reflectance variations of the atmosphere and land surface (Danaher, 2002). The method combines a simple top-of atmosphere (TOA) reflectance adjustment with a modified version of the Walthall empirical BRDF model (Walthall et al., 1985). The model parameters were derived from an overlapping sequence of Landsat 7 ETM+ images and were applied to produce spatially matched mosaics of Landsat ETM+ and TM imagery (Danaher, 2002).

The training dataset for estimating FPC from these data was compiled from basal area data collected between 1996 and 1999 from 1630 sites uniformly distributed throughout Queensland in stands of contiguous mature remnant forest,

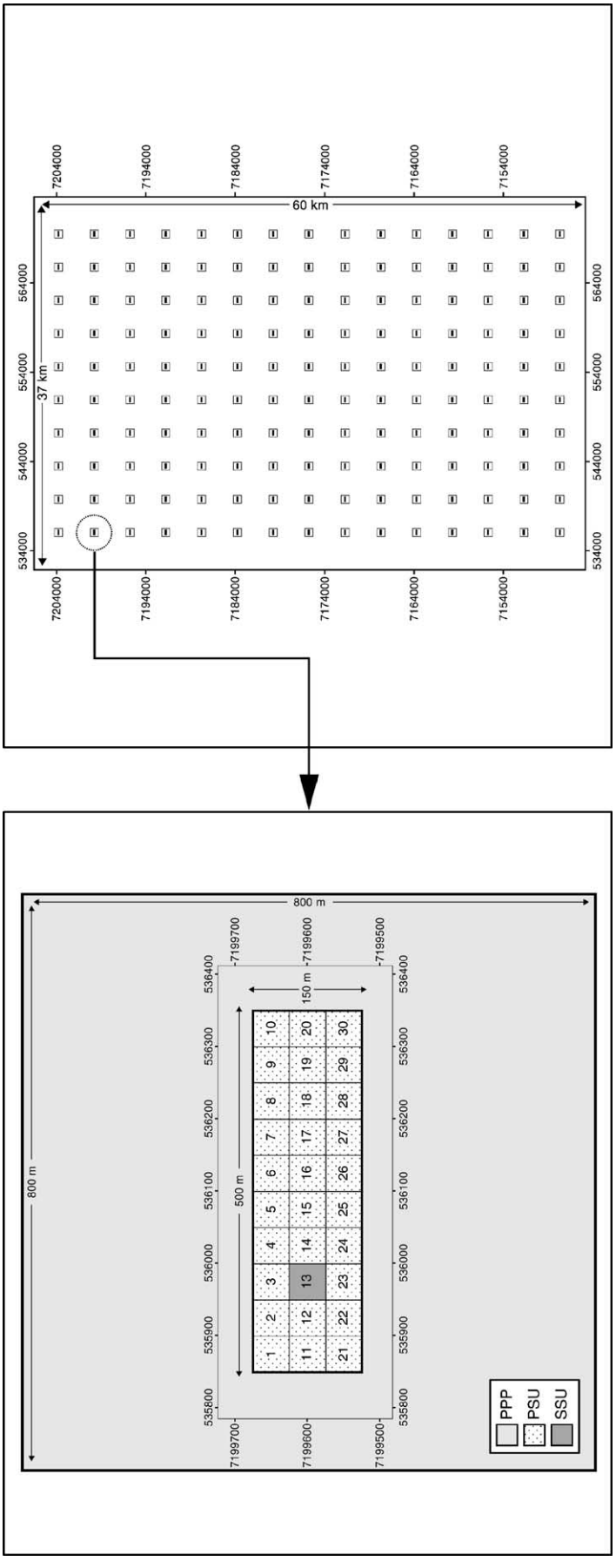

Fig. 3. The layout of the PSU and SSU grid.

ranging from very sparse woodland to dense rainforest. Basal area was calculated from an average of 5 recordings, using a calibrated optical wedge (Dilworth & Bell, 1971). Overstorey FPC was coincidentally measured for the observed ranged of basal area at 236 of these sites using the gimballed cross hair sighting tube method. For further details on the sampling design and field procedures used see Danaher et al. (2004), Hassett et al. (2000) and Kuhnell et al. (1998). To ensure sufficient representation of the range of background reflectance over the State, additional sites with zero woody FPC that covered the main soil types were collected through interpretation of available large scale aerial photography. Sites with both FPC and basal area measurements were used to develop a stand scale allometric relationship (R^2=0.82, Residual Mean Square Error (RMSE)=6.93, N=236) expressed as a general linear model with a binomial error distribution and a log link such that:

$$\mathrm{FPC} = 100 \cdot \left(1 - e^{-0.0355 \cdot BA}\right) \quad (1)$$

where BA represents basal area. Fig. 4 shows this asymptotic increase in FPC with basal area, with confidence intervals. Direct relationships between Landsat sensor data and basal area were not considered, as retrieval ideally requires a sensor that observes the three-dimensional structural of forests. Therefore, FPC was preferentially used as it is regarded as an attribute that can be more directly retrieved from Landsat data, as this sensor views the canopy in two dimensions. The RMSE of the relationship (9.68) is difficult to decompose. The relationship is for mature undisturbed vegetation only and much of the observed variation is arguably attributable to measurement error in basal area and a more binomial variation than expected for FPC. The relationship would be expected to vary between species according to foliage clumping and leaf angle distribution, although these data are not available to support an analysis. There is, however, no clear correspondence between dominant genus and the observed variability, suggesting that major differences in structure, such as those observed between Eucalyptus and Acacia species, are not the primary source of variability and other factors (e.g., measurement error) are more likely to be responsible.

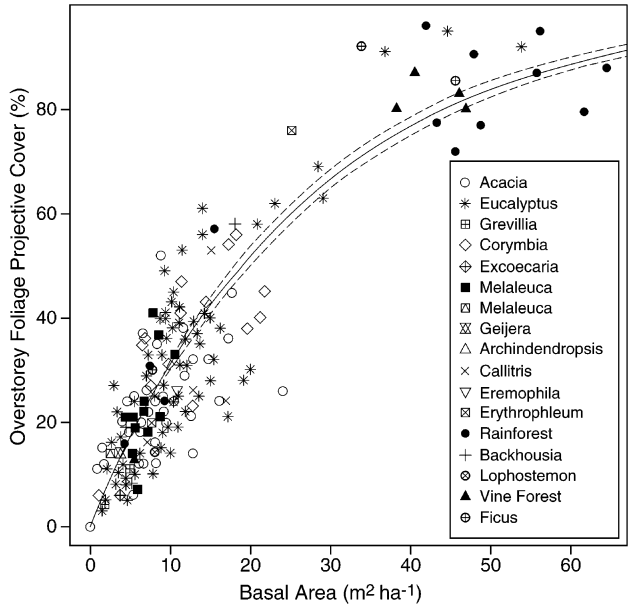

Fig. 4. The stand scale allometric relationship between basal area and overstorey FPC. The legend indicates dominant genus but where not recorded, the plant community is listed (e.g., rainforest, vine forest). The dashed lines are the confidence intervals.

Landsat sensor band 2–7 reflectance data were extracted from 3 × 3 pixel windows centred on each of the 1630 field site locations for the three SLATS scenes closest to the field data acquisition date for each site and averaged. The spatial aggregation was undertaken to match the spatial scale of the field sites, and the temporal averaging was performed to minimise the effect of known phenological variations in overstorey FPC that were not accounted for by Eq. (1) (Hassett et al., 2000). Training datasets were developed separately for Landsat TM and ETM+ because of known differences in bandwidth and the spectral response of these sensors (NASA, 2004). Band 1 reflectance data were excluded as scene-to-scene differences in radiometrically corrected data were significantly higher than for all other bands (Danaher, 2002). Long-term average vapour pressure deficit (VPD; Jeffrey et al., 2001) data interpolated from meteorological station measurements were also included as a variable because the evaporative potential of the atmosphere is correlated with FPC (Specht & Specht, 1999). Data affected by cloud or land cover change were removed from the training dataset. Changes in basal area between the date of site measurement and image acquisition dates were assumed negligible, particularly as all field sites were located in mature undisturbed vegetation.

For this study, multiple linear regression between field-based estimates and the data associated with each of the Landsat reflectance channels was used for determining allometric FPC. In the presence of representative and appropriately sampled training data, this technique has been shown to perform as well as non-linear techniques such as regression trees and artificial neural networks (e.g., De Fries et al., 1997; Fernandes et al., 2004), although comparison of techniques is yet to be completed for the study site. A disadvantage of this technique, as applied in this study, is that the contribution of individual bands is difficult to determine due to multi-collinearity. However, the objective here was simply to achieve the best possible predictive accuracy for multiple Landsat sensors in the presence of extensive soil colour and floristic variation. The regression model was developed using all-subsets multiple linear regression such that:

$$y = \alpha + \beta_i x_a + \beta_2 x_2 \ldots \beta_n x_n + \varepsilon \quad (2)$$

where α is the intercept, ε is the error term, β_i is the ith coefficient of n terms and x_i represents the input terms consisting of Landsat bands 2–7, interactions (e.g., Band 3 × Band 5) and VPD (Danaher et al., 2004). Standard selection criteria was used for the all-subsets variable selection and included maximising the adjusted R^2 and minimising the Mallows' C_p statistic (Danaher et al., 2004). The adjusted R^2 is a modified version of the R^2 statistic that takes into account the

reduced degrees of freedom resulting from the inclusion of more terms in the regression model

$$R^2_{\text{Adjusted}} = 1 - \frac{(n-1)(1-r^2)}{n-t}. \quad (3)$$

The Mallows' C_p statistic, which provides a measure of the trade-off between bias resulting from the exclusion of important terms and extra variance associated with the inclusion of too many, is given as:

$$C_p = \frac{\text{SSE}}{\sigma^2_{\text{exp}}} - (n-2t) \quad (4)$$

where SSE is the sum of the squared error between the observed and predicted values of y and σ^2_{exp} is the expected value of the residual variance. As there was no a priori knowledge of σ^2_{exp}, the value was set as the residual variance of the regression model with all possible terms. The use of these statistics in multiple regression analysis of remotely sensed data is discussed by Salvador and Pons (1998).

The resulting candidate models were assessed by 5-fold cross-validation to ensure the model predictions were not spurious (Table 1). Here, the accuracy of the regression models are reasonable, with an adjusted R^2 greater than or equal to 0.80 and a RMSE of less than 10.0 for both the models and the cross-validation results. The high number of terms was accepted due to the complexity of the soil and overstorey spectral response within Queensland, the high number of observations (N), and cross-validation results. The differences between the terms selected for the Landsat-5 TM and Landsat-7 ETM+ models were attributed to the minor differences of spectral response and bandwidth between the two sensors. An evaluation of regression modelling strategies applicable to the derivation of basal area and FPC from Landsat sensor data over large areas together with state-wide validation of resulting predictions using a combination of field and Light Detection and Ranging (LiDAR) data is currently is progress by SLATS.

For use with the 2000 AIRSAR data, estimates of FPC were generated for the Injune study area by applying the techniques above to Landsat-7 ETM+ data acquired on 2nd September 2000. A good correspondence between FPC

Table 1
Results of the models selected using all-subsets multiple linear regression

Results		Landsat-5 TM	Landsat-7 ETM+
Model	N	2342	2402
	Adjusted R^2	0.82	0.80
	S.E.	7.98	8.25
Cross-validation	Mean Adjusted R^2	0.81	0.80
	Mean S.E.	8.14	8.31
Model terms	Single Band	$\sqrt{B3}$, $\sqrt{B4}$, $\sqrt{B5}$, $\sqrt{B7}$	$\sqrt{B3}$, $\sqrt{B4}$, $\sqrt{B5}$, $\sqrt{B7}$
		VPD^{-1}	VPD^{-1}
	Interaction	$\sqrt{B2B5}$, $\sqrt{B3B5}$, $\sqrt{B3B7}$, $\sqrt{B4B5}$, $\sqrt{B4B7}$	$\sqrt{B2B4}$, $\sqrt{B3B5}$, $\sqrt{B3B7}$, $\sqrt{B4B5}$, $\sqrt{B4B7}$, $\sqrt{B5B7}$

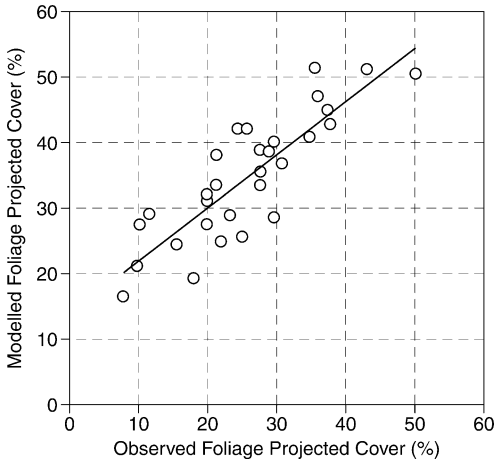

Fig. 5. Comparison of field measured (observed) FPC and modelled allometric FPC. Landsat-7 ETM+ data acquired on 2nd September 2000 over Injune were used as input to the FPC estimation algorithm.

modelled from the stand scale allometric equation with that measured in selected SSUs during a field campaign to Injune (Lucas et al., 2004) was observed (R^2=0.73, RMSE=4.28), although the former was consistently greater (Fig. 5). The reasons for this are (a) the field observations do not include perennial foliage less than 2 m above the ground, to which the Landsat-7 ETM+ derived estimates are still sensitive and (b) FPC was recorded along three 50-m transects in structurally heterogeneous forests; by shifting the transect location, some differences in FPC would have been observed. Despite these limitations, it was considered that the SLATS allometric FPC predictions were sufficiently accurate for application within the study site. AIRSAR C-, L- and P-band $\sigma°$ data (all polarisations) as well as Landsat-derived FPC were then extracted independently from each SSU within PSU column 3 where areas of woody regrowth dominated by Brigalow as well as a range of other forest types were evident. Scatterplots relating FPC and SAR $\sigma°$ for the different forest types were then generated with a view to fitting a regression line for all types combined. Extensive regrowth was also evident to the south of the PSU, although LSP were not available for this area.

5. Results

5.1. Relationships between SAR $\sigma°$ and FPC

For the majority of forests, most of which were remnant, an increase in FPC with SAR $\sigma°$ was observed at all frequencies and polarisations which could be described using a non-linear regression curve, as illustrated for Column 3 (Fig. 6). At C-band, the increase in $\sigma°$ with FPC was particularly evident at HV polarisations as were differences between communities, with those dominated by *C. glaucophylla* and *E. melanphloia* typically supporting higher values. This increase was evident for all 10 PSU columns suggesting opportunities for species/community discrimination and mapping. This is the focus of a forthcoming paper.

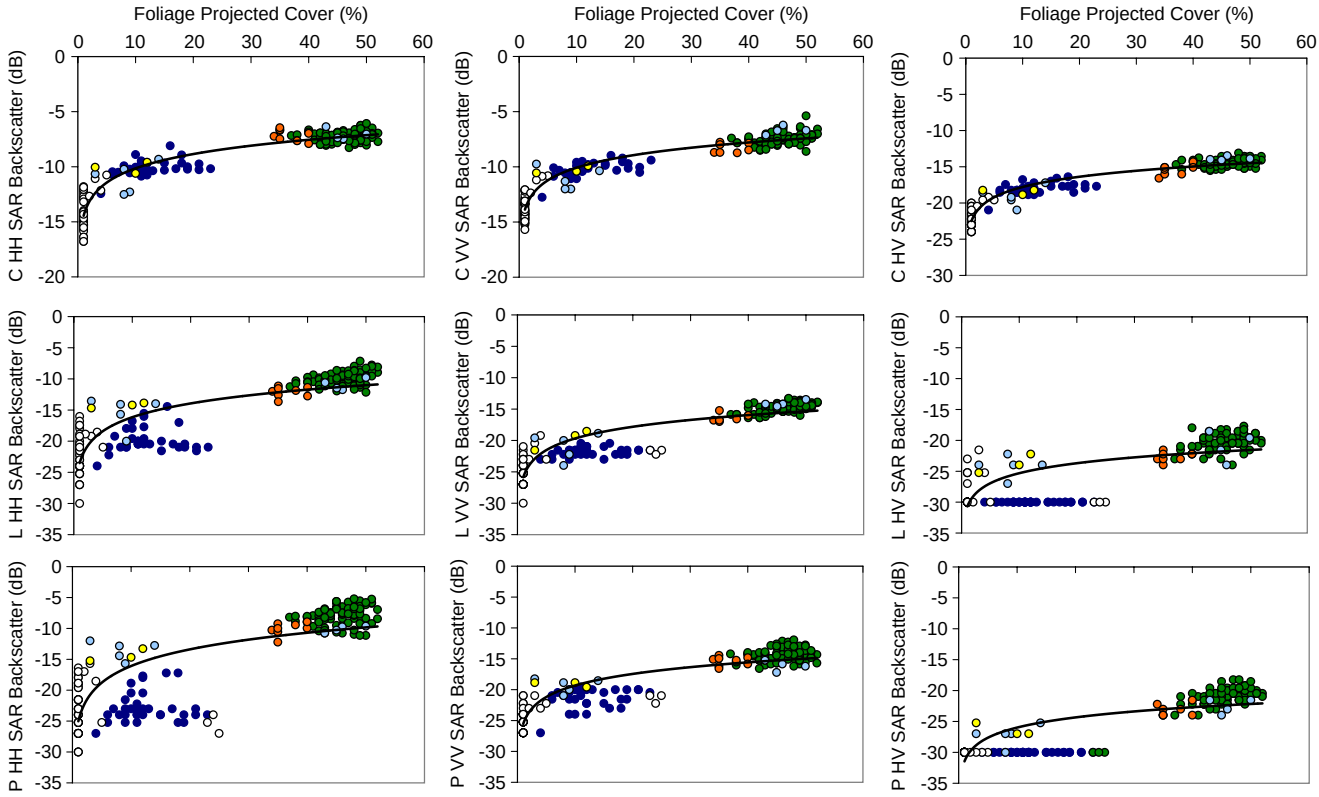

Fig. 6. Relationships between C-band, L-band and P-band SAR σ° and FPC. Note that the SAR σ° in all channels increases with FPC in all forests except those associated with Brigalow (*Acacia harpophylla*; dark blue) where L-band and P-band σ° remains low or insignificant. The different marker colours are associated with non-forest (clear) and communities containing *C. glaucophylla* (green), *E. mitchelli* (yellow), *E. melanaphloia* (cyan) and *E. populnea* (orange).

Within column 3, extensive areas of Brigalow-dominated regrowth were evident and supported an FPC of up to 53%. At L-band, and particularly at P-band, σ° from this regrowth generally did not increase above that of the non-vegetated areas and differences from the fitted non-linear regression curve were greatest at HH polarisations. At L-band and P-band HV polarisation, σ° from the regrowth was below the sensitivity level of the AIRSAR. These low levels of σ° were attributable to the absence of woody components of sufficient size to evoke a discernible double bounce scattering towards the sensor at these lower frequencies, despite the high density of stems and branches. As a result, specular scattering from the ground and away from the sensor dominates. By contrast, σ° from low biomass stands dominated by *E. mitchelli*, *E. melanaphloia* and other *Acacia* species, increased with FPC. Within these forests, L-band and P-band microwaves were considered to interact with the larger (albeit fewer) trunks and branches of individual trees because of their greater size and a greater return was therefore recorded. SAR σ° from some areas of Brigalow was equivalent to these low biomass stands, suggesting a similarity in the size class distributions of woody components or co-existence within stands with larger trees of the same or other species contained.

Other areas of Brigalow regrowth were known to occur within the study area, particularly to the south of the PSU grid. Within the colour composite of the AIRSAR C-band, L-band and P-band Total Power images (in red, green and blue), these areas were noticeable as they exhibited a distinct red colour (Fig. 7), which was attributable to C-band σ° (in red) being similar for both Brigalow and remnant forests but L-band and particularly P-band σ° from Brigalow being comparatively lower than that of remnant forest and typically equivalent to or only slightly above that of non-forest. The greatest contrast between regrowth and remnant forest was observed at P-band.

5.1.1. Mapping woody regrowth using low frequency SAR and FPC

For mapping woody (typically remnant) vegetation in Queensland, an FPC threshold approximating 12% is typically used, although this may vary by several percent (Henry et al., 2002). Areas of regrowth can, however, also support an FPC exceeding 12% and even approaching 40–60%, because of the large number of crowns and the dense foliage cover. As such, these forests are often incorrectly assumed to be relatively mature forest, which support a high basal area and biomass, and are hence mapped as remnant vegetation. Regrowth and remnant forests also support a C-band backscatter (all polarisations) that is similar. By contrast, regrowth forests support a low L-band and particularly P-band σ° compared to remnant vegetation that is equivalent to non-forest. Therefore, by applying simple thresholds to these low frequency SAR data (e.g. $<=\sim 14$ dB to L-band HH data) in areas where the FPC exceeds 12%, areas of regrowth can be mapped as separate from remnant forests (and non-forest). Regrowth forests containing a fewer number of trees of larger stem dimensions,

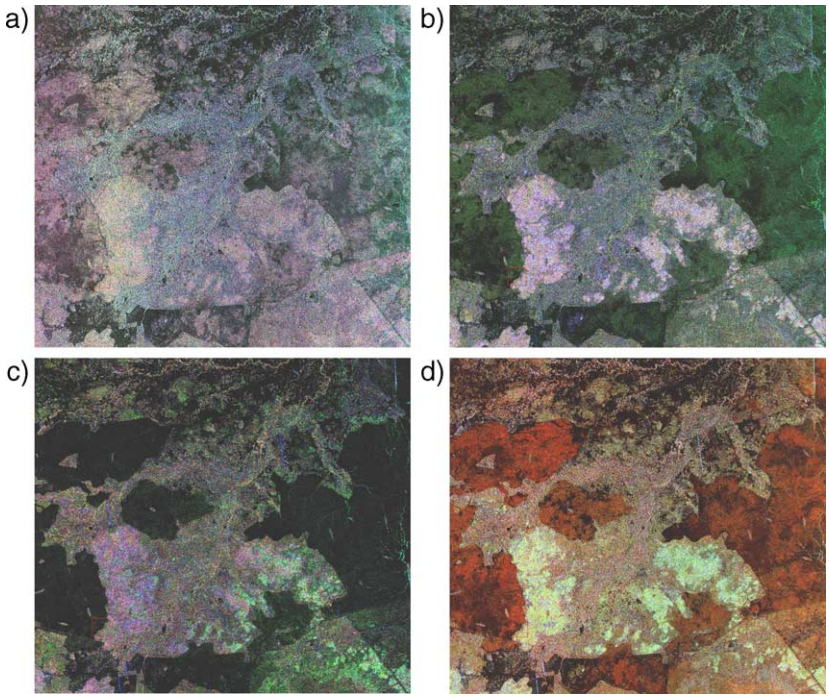

Fig. 7. A comparison of (a) C-band, (b) L-band and (c) P-band σ° (HV, VV and HH in RGB) data and (d) total power (TP; C-band, L-band and P-band in RGB) illustrating the reducing σ° from BGL regrowth with decreasing frequency. Areas of Brigalow regrowth are particularly evident (in red) within the TP image. The scene covers an area of approximately 10×10 km and occurs to the south of the main PSU grid.

which are typically at a more advanced stage of regeneration, can also be distinguished from Brigalow-type regrowth although less so from remnant forest. Although either L-band and P-band SAR data could be used for mapping, attention turned to the use of L-band SAR as these data are more likely to be available on a regional basis following the launch of Japan's ALOS PALSAR in 2006. Regrowth maps were therefore generated based on either L-band HH or HV SAR data, as the distribution of the mapped areas was similar regardless of the polarisation used. Similar maps were also able to be generated using P-band data. Although regional data are provided by the RADARSAT and ENVISAT Advanced SAR (ASAR), C-band backscatter data were only considered useful for mapping regrowth if used as a substitute for Landsat FPC data. Hence, no further discussion on their utility is warranted.

Assessing the validity of the regrowth maps derived from AIRSAR L-band and FPC data was difficult given that woody regrowth is not discriminated from remnant vegetation in the woody vegetation (i.e., forest) mapping conducted by SLATS. Two alternative approaches were therefore considered. In the first, Brigalow regrowth were identified with the HyMap imagery as vegetation typically located within the centres of previously cleared areas and supporting a high density of small, low and closely packed crowns (Fig. 8a). Within the Landsat FPC data, and at 25 m spatial resolution, these areas typically supported an FPC of between 12% and ~53% (Fig. 8b), although the FPC of very young stands was often below that associated with woody vegetation. Compared to bare ground, σ° was greater within AIRSAR C-band data but at L-band and P-band, was similar and well below that of the remnant forest (Fig. 8c). Areas of Brigalow were delineated within the Hymap data using supervised nearest neighbour classification techniques developed within Ecognition and then overlain onto the SAR-derived regrowth classification, as shown in Fig. 8d. For all areas of regrowth classified within six HyMap strips, of which the image illustrated is a small subset, a very close correspondence between regrowth mapped using the SAR data was observed.

In the second case, a land cover map for 2000 showing classes of non-forest, regrowth and remnant forest (Fig. 9a) was generated from the SLATS 1991 Landsat TM-derived FPC data, SLATS 1991–1995, 1995–1997, 1997–1999 vegetation change datasets (categorised into forest or non-forest) and the Landsat ETM+ -derived FPC data for 2000. Using the FPC grids from 1991 and 2000, forest (including regrowth) and non-forest were mapped as areas having an FPC greater and less than 12% respectively. Areas identified as non-forest in 1991 or mapped as change from either forest (e.g., cleared) or non-forest (i.e., to a different land cover or use) in the subsequent SLATS vegetation change datasets but as forest in 2000 were then associated with regrowth. Change was mapped even though the clearance of vegetation was incomplete in some areas (e.g., because of stem injection or selective cutting of trees). The resulting map was then compared with the map of regrowth generated using Landsat FPC data and AIRSAR L-band HH for 2000 (Fig. 8b), both visually and quantitatively (Table 2).

When comparing the datasets, it was necessarily assumed that the map generated using the time-series dataset was the ground truth as no other datasets of regrowth with the same spatial coverage were available. Initially, a close correspondence (>90%) between the areas mapped as forest and non-forest was observed which translated into an overall correspondence of 87.8%. However, only 57.4% of the regrowth

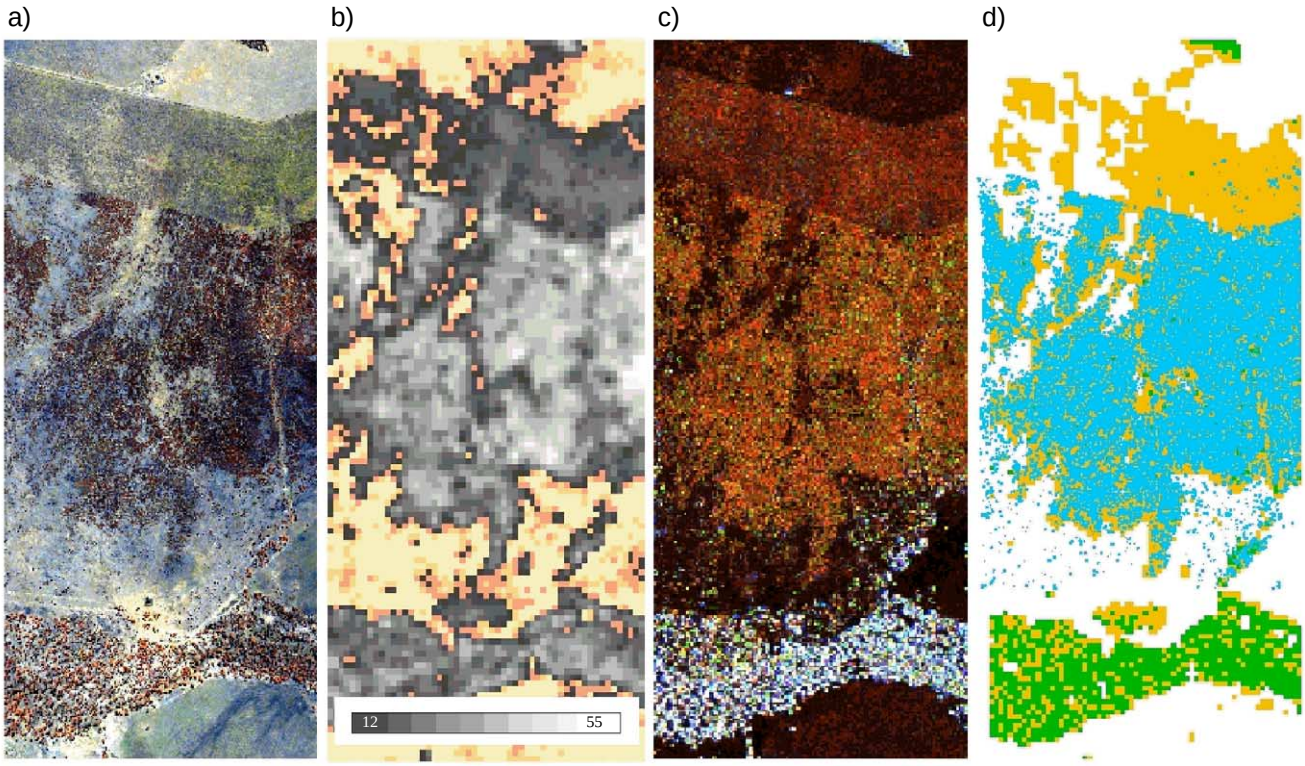

Fig. 8. (a) HyMap image showing areas of regrowth with PSU C3, (b) FPC image of Brigalow regrowth representing an FPC of up to 53% (areas below 12% are coloured), (c) regrowth as observed using a combination of C-, L- and P-band Total Power (in RGB) and (d) the mapped area of Brigalow regrowth (orange) and remnant forest (green) The area in blue is the area of regrowth observed in (a) overlain onto the classification.

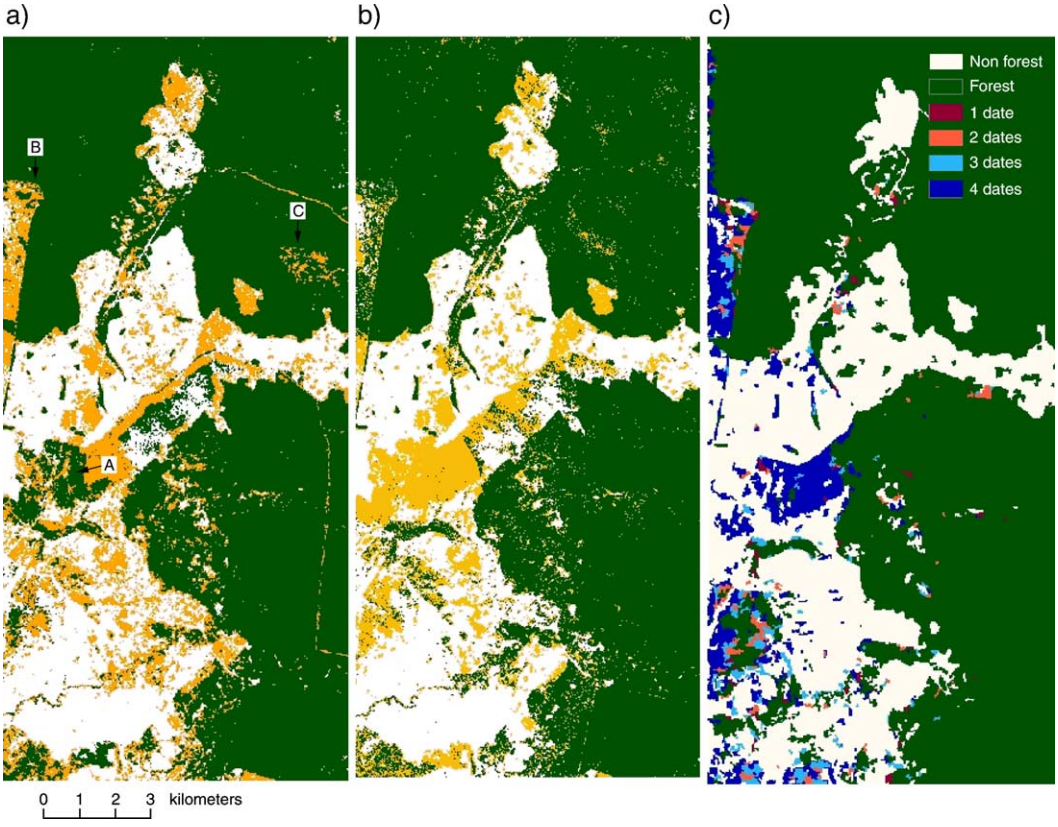

Fig. 9. (a) Classification of woody regrowth (orange), forest (green) and non-forest (white) based on time-series comparison of Landsat-derived land cover datasets. A, B and C represent misclassified areas. (b) Classification of woody regrowth (orange), forest (green) and non-forest (white) using Landsat-derived FPC and AIRSAR L-band HH SAR thresholds. (c) Areas of regrowth mapped using JERS-1 SAR data acquired during 1994–1995.

Table 2
Correspondence (in pixels) between land cover mapped (in 2000) through comparisons of Landsat-derived FPC and AIRSAR L-band HH SAR data classification with a) the original and b) corrected time-series classification of Landsat sensor data

		AIRSAR				
		Forest	Non-forest	Regrowth	Sum	%
(a)						
Time-series	Forest	1,126,942	23,275	80,794	1,231,011	91.5
	Non-forest	6,506	499,590	18,750	524,846	95.2
	Regrowth	89,641	28,553	159,319	277,513	57.4
	Sum	1,223,089	551,418	258,863	2,033,370	
	%	92.1	90.6	61.6		87.8
(b)						
Time-series	Forest	1,143,629	23,275	32,525	1,199,429	95.3
	Non-forest	6,506	499,590	18,750	524,846	95.2
	Regrowth	72,954	28,553	207,588	309,095	67.2
	Sum	1,223,089	551,418	258,863	2,033,370	
	%	93.5	90.6	80.2		91.0

identified within the time-series was mapped using the AIRSAR/FPC data whilst 61.6% of the regrowth mapped using the AIRSAR/FPC data was similarly mapped using the time-series (Table 2a). However, when the validity of the time-series map as ground truth for regrowth extent was assessed by comparing against the distribution of Brigalow observed with the HyMap strips, 3.9% (48,269 10-m pixels) of the forest class were identified as regrowth (see A in Fig. 9a as an example). Therefore, the time-series map was amended by reallocating the forest areas that were incorrectly classified to regrowth. Similarly, the HyMap data suggested that approximately 7% of the regrowth mapped using the time-series datasets had occurred in areas where some trees had been left standing (B), whilst a further 2.5% were associated with a fire event within the remnant forest (C). Although regrowth did occur in the first case, the presence of trees with larger branches and trunks resulted in increased double bounce scattering to the sensor and hence only patches of regrowth between these trees were mapped using the AIRSAR/FPC data combination, thereby resulting in this area being classified largely as forest. Even so, a change event was identified using the time-series and hence regrowth across the area was inferred. However, in the burnt area, the high L-band backscatter (all polarisations) suggested that no changes in large woody biomass had occurred and that change was only detected in the time-series because of a temporary loss of leaf cover (and hence FPC) during the fire. When these corrections to the time-series map were implemented, 67.2% of the regrowth mapped in the corrected time-series was similarly classified using the AIRSAR FPC and 80.2% of the regrowth mapped using the AIRSAR FPC was classified as such using the time-series (Table 2b), thereby giving an average correspondence of 73.7%. In all cases, the accuracy of the AIRSAR/FPC classification is considered to be higher for several reasons. Some areas of regeneration and also open understorey within the undisturbed forest were identified using the AIRSAR/FPC combination, but were amalgamated within the forest class of the time-series classification. Compensating for these smaller areas was difficult because of uncertainty in the interpretation of the HyMap data. Adjustments to the AIRSAR/FPC classifications were also only made for areas where large discrepancies were observed, and smaller errors associated with the time-series classification and geometric correction errors could not be accounted for.

These observations confirm that the integration of FPC and L-band SAR can be used to map regrowth, but mainly those stands that are structurally homogeneous and do not contain trunks above a certain size class, as typified by regenerating Brigalow. Where larger trees remain or establish within an area, the mapping is less successful but detection of regeneration within gaps or even beneath open canopies allows areas affected by partial clearance events or those in more advanced stages of regeneration to be identified. The discrepancies observed in the comparison can therefore be explained and also suggest that the SAR data can be investigated further to better understand the dynamics of clearing and regeneration, including ingrowth within existing forest areas. The integration of FPC and low frequency SAR, which relies on single-date image combinations, is also more successful at mapping regrowth compared to the time-series analysis of Landsat sensor classifications and is certainly less demanding of time and data.

5.2. Use of JERS-1 SAR data for mapping woody regrowth

A limitation of AIRSAR data for regrowth mapping is that data are only acquired during specialised missions (e.g., the PACRIM II) and the extent of coverage is relatively limited. For this reason, the integration of historical Japanese Earth Resources Satellite (JERS-1) SAR and Landsat TM-derived FPC data acquired over the Injune study area was investigated for their potential to map woody regrowth. These data were acquired on four dates between 1994 and 1995 covering both the wet and dry seasons. Acquisitions occurred over a period where no rainfall was recorded with the exception of the 12th August 1994, where 15 mm was noted on the previous day (Bureau of Meteorology, 1996). For the same period, FPC estimates were generated by SLATS based on the 1995 Landsat ETM+ image and applying the procedure described above.

As with the previous analysis of AIRSAR and FPC data for 2000, areas of woody regrowth were mapped using a FPC threshold of $\geq$12%. The JERS-1 SAR L-band HH threshold for discriminating remnant forest from regrowth was established for the scene of 29th June 1994 as approximating −14 dB. To map a similar area (assuming that no clearing or regenerating had occurred over the 14-month period) within the other scenes, the thresholds listed in Table 3 were required. A similar threshold of

Table 3
JERS-1 SAR L-band HH σ° thresholds applied for the mapping of woody regrowth

Image acquisition date	L-band HH threshold
29 June 1994	−14.0
12 August 1994	−11.3
16 June 1994	−13.4
12 September 1995	−13.8

Note that an FPC threshold of 12% was also used.

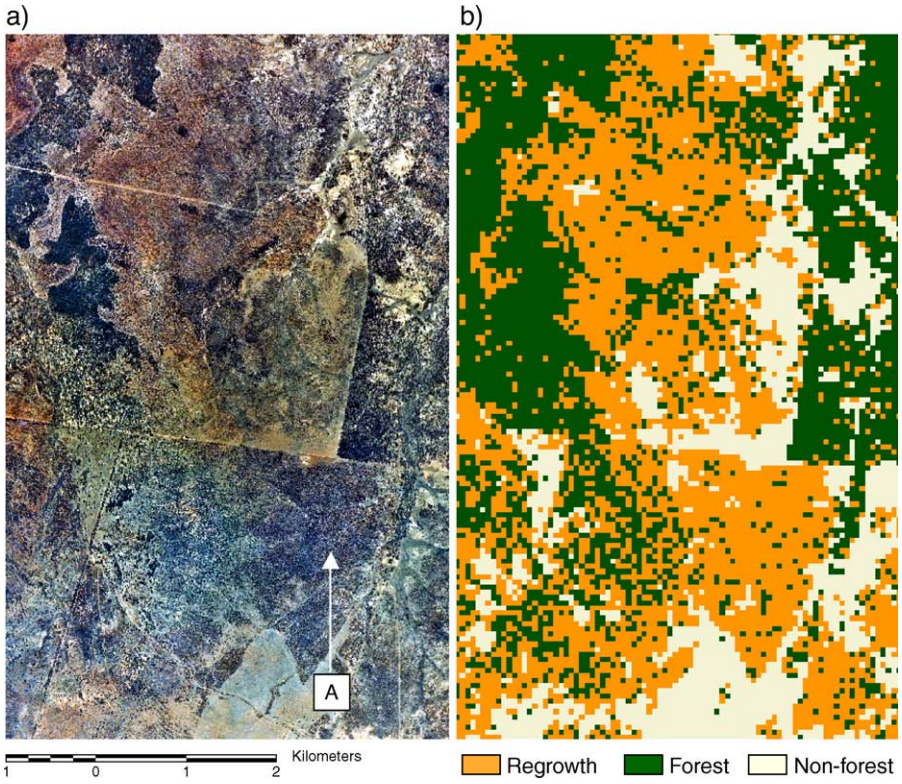

Fig. 10. (a) 1:40,000 colour aerial photography acquired on 29th June 1995, showing areas of regrowth (including A) and (b) the area of regrowth mapped using 1995 JERS-1 SAR L-band HH and FPC data. A close correspondence with areas mapped using Landsat FPC/JERS-1 SAR L-band HH and observed within the photography is evident. Much of this area was classified as remnant vegetation using a threshold of FPC data alone.

−13.4 and −13.8 dB was used for the 16th June 1994 and 12th September 1995 respectively, although a higher threshold of −11.3 dB was necessary to map regrowth from the scene acquired on the 12th August 1994. This was attributed to greater moisture on the surface of the vegetation and ground surface as a result of the rainfall event. The areas mapped using the four JERS-1 SAR scenes were compared and, in general, similar areas were mapped on all dates, with differences attributed, in part, to temporal changes in regrowth cover (Fig. 9c).

As with 2000, no regrowth maps were produced for 1995 by SLATS. The classifications generated using JERS-1 SAR L-band data and FPC were therefore necessarily compared with 1:40,000 colour aerial photography acquired to the west of the study area on 29th June 1995 (Fig. 10). Interpretation of the aerial photography suggested that both old and young stands of Brigalow regrowth were being mapped. This interpretation was supported by comparison with Landsat-derived maps of regrowth generated for 2000, where much of the regrowth identified in 2000 was mapped as such using the 1995 JERS-1 SAR (Fig. 9a).

6. SAR backscatter modelling

6.1. Model parameterisation

To better understand the reduced SAR σ° from Brigalow regrowth at progressively lower frequencies, a forward wave scattering model based on that of Durden et al. (1989) was parameterised such that the effect of changing stem size and density as well as leaf amount on the overall σ° and the contribution of the differing scattering mechanisms (e.g., single bounce, double bounce or volume scattering) could be investigated. The parameters used were not intended to represent an actual forest, as this is difficult given the complexity of the regrowth, particularly in disturbed environments, but rather to illustrate the significance of changes in forest structure on the SAR σ° as the regeneration proceeds.

The two-layered model of Durden et al. (1989) requires that, for decurrent trees (i.e., those of a form typical to *Eucalyptus* or temperate deciduous species and including Brigalow), branches and leaves are contained solely in the upper layer whilst the lower layer consists of stems, which are modelled as randomly located vertical dielectric cylinders. The depth of the two layers varies depending upon the vertical space occupied by the canopy relative to total tree height and was determined using an empirical relationship established between field-based measurements of the top height and crown depth (to the first leafing branch) taken from Brigalow trees at Injune. Branches are represented by finite dielectric cylinders which correspond to a $\sin^4\alpha$ distribution, such that α represents the angle about the mean orientation angle with respect to the vertical. The ground is assumed to be a Bragg rough surface characterised by a first order small perturbation model and scattering from each layer is calculated using a first order (distorted Born) approximation. The wave attenuation through the branch and trunk layers is accounted for by averaging the elements of the forward scattering amplitude matrix over all cylinder orientations, thereby amounting to a distorted Born approximation for the

Table 4
Allometric equations for the estimation of component biomass (g) for Brigalow (for trees <5 m in height) based on height (cm)

Biomass component	a	b	se$b$	s^2	R^2
Leaf	−2.84	1.629	0.259	0.493	0.6
Branch	−4.056	1.805	0.233	0.401	0.69
Stem bark	−8.332	2.579	0.232	0.396	0.82
Stem wood	−8.009	2.621	0.2	0.296	0.87
All stem	−7.49	2.611	0.206	0.314	0.86
Total	−4.303	2.15	0.205	0.311	0.86

Equations are of the form biomass $= e^{(a+b\ln X)}e^{(s2/2)}$.

total effect of the vegetation layer on $\sigma°$. The model was parameterised using forest inventory data, leaf measurements, and allometric equations specific to Brigalow that separately estimated the component (leaf, branch and trunk) biomass of individual trees (Harrington, 1979; Scanlan, 1991; Table 4). The method of parameterisation was similar to that described in Lucas et al. (2004) and Liang et al. (2005).

For estimating the component biomass of Brigalow, the equations of Scanlan (1991) rather than Harrington (1979) were used as the former focused on stands regenerating on abandoned pastures. Scanlan (1991) harvested 29 individuals (ranging in height from 0.45 to 5 m) from six separate stands near Theodore, central Queensland (24°50′S, 149°48′ E) and established separate equations for estimating leaf, branch and stem (bark, wood and total) biomass (g) from both circumference (mm) and height (cm) measurements. For this study, the biomass prediction equations using height as the independent

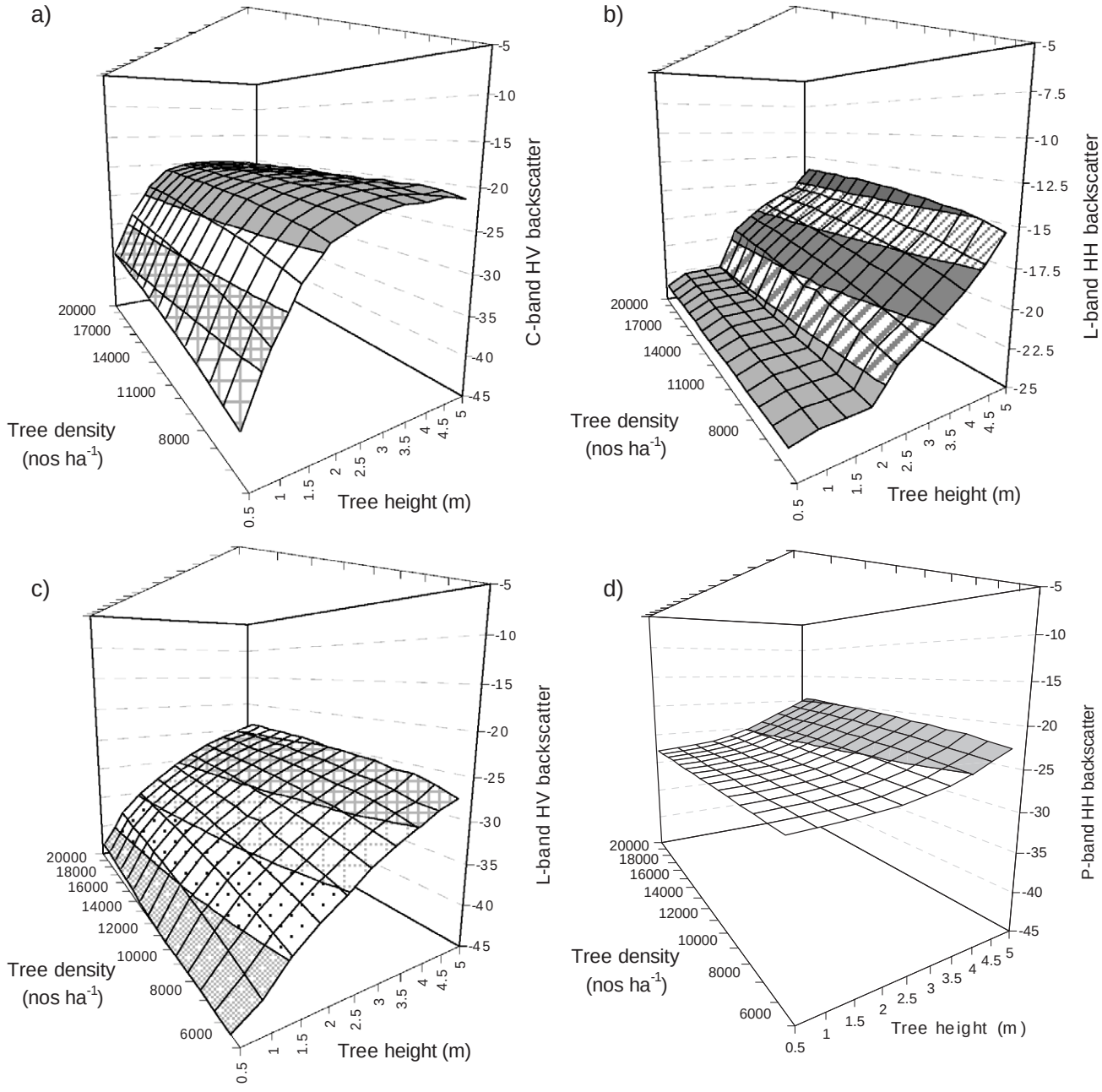

Fig. 11. Simulated SAR $\sigma°$ at (a) C-band HV, (b) L-band HH, (c) L-band HV and (d) P-band HH.

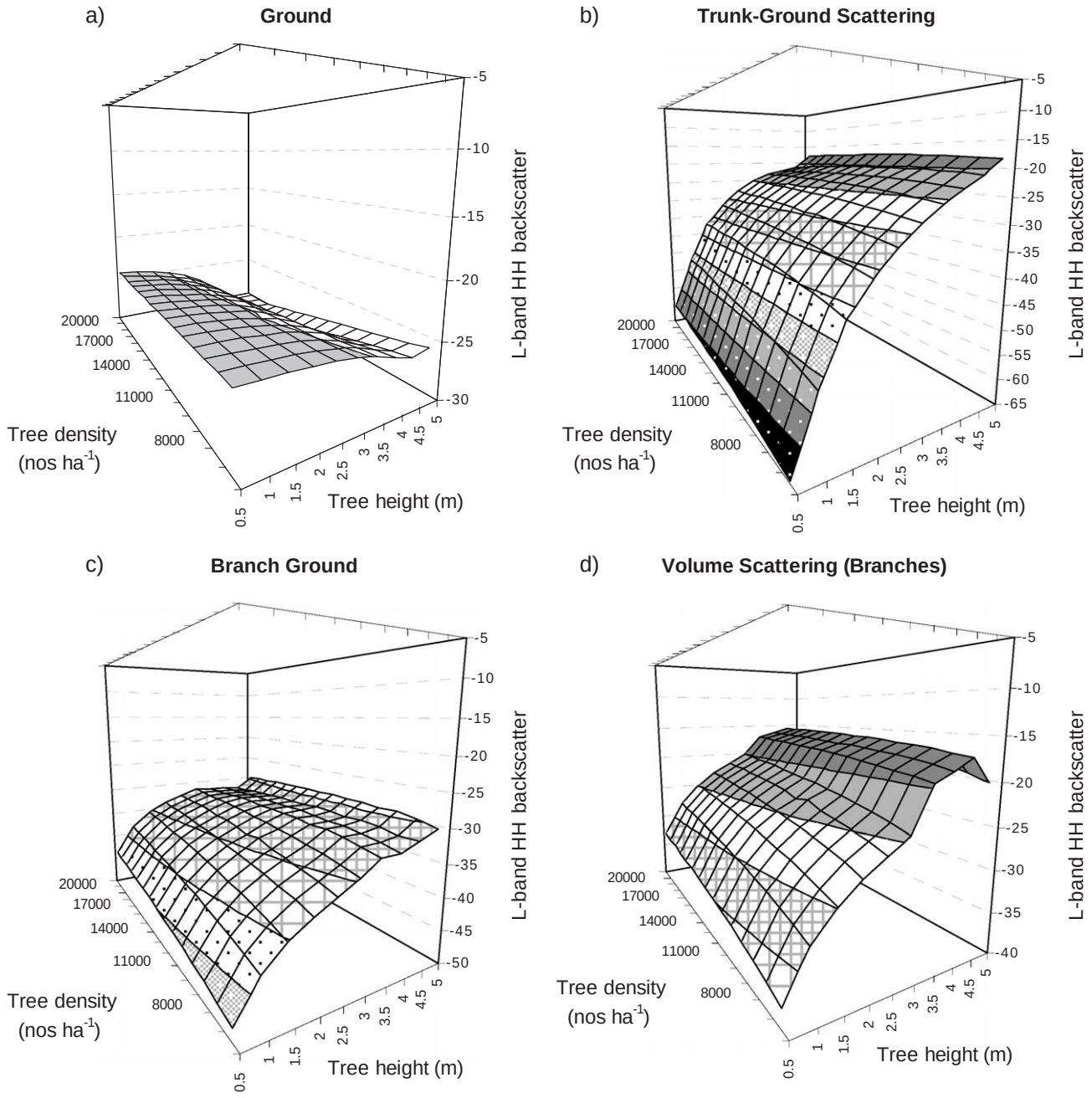

Fig. 12. Simulated contributions of the different scattering mechanisms to total L-band σ°, with a-d representing the contribution of the different scattering mechanisms.

variable were utilised (Table 4). For the estimation, the residual mean square of the regression was used to calculate the bias correction factor ($e^{(s2/2)}$; Baskerville, 1972).

For modelling, the parameterisation necessarily assumed that the stems were homogeneous in terms of their size and spatial distribution. Each regrowth stand therefore contained trees of the same height, which was varied from 0.5 m to 5 m (within the range of the allometric equations), and stem diameter, which varied from 0.7 to 4.6 cm and was approximated from height. Brigalow exhibits a branching habit, particularly when coppiced, and the number and size of branches emanating from the trunk was determined as proportional to branch biomass and crown depth. Based on field measurements, leaf weight, radius (average of length and width) and thickness were assigned values of 0.27 g, 2.7 cm and 0.43 mm, respectively, and kept constant. Branching angle was set at 31° from vertical, as determined from digital photographs of individual trees, with an exponent of 1 to allow variation in orientation. Then, for each stand, tree density was varied from 6000 to 20,000 stems ha^{-1} at intervals of 1000 stems ha^{-1}, although a maximum total biomass limit (of ~20 Mg ha^{-1}) was imposed on each stand. For each simulation, the total SAR σ° at C-band, L-band and P-band was calculated, together with the contribution of the differing scattering mechanisms (volume, branch-ground, trunk-ground and ground) to the total σ° at C-, L- and P-band (all polarisations), although results largely relevant to current

and near future spaceborne SAR are reported here. The incidence angle was set at 45°.

6.1.1. Scattering behaviour

Previous studies at Injune (Lucas et al., 2004) have indicated a close relationship between C-band HV σ° and the biomass of the leaves and small (<1 cm diameter) branches combined. Simulations at C-band HV for Brigalow stands also confirmed an increase in σ° from the early stages of regeneration to an asymptote approximating −20 dB (Fig. 11a). By contrast, simulations at L-band HH suggested that σ° remained relatively similar (at less than ~22 dB) until stem height exceeded 2.0 m, at which point a rapid increase in σ° was observed (Fig. 11b). Only slight increases in L-band HH σ° were observed for stands of height less than 2 m. Simulations at L-band HV suggested σ° increased with both height and density but was generally below −25 dB indicating low sensitivity (Fig. 11c). However, it can be expected that L-band HV σ° will increase as the size and density of the branches increases, due to greater sensitivity to these components (Lucas et al., 2004). Simulations at P-band HH generally resulted in small values of σ° until stands approached 4–5 m (Fig. 11d), at which point a slight increase was evident. Simulated P-band HV σ° was insignificant for the stands considered.

To better understand the influence of the changing structure of Brigalow regrowth on microwave interaction, the contribution of the different scattering mechanisms to the total σ° was investigated, focusing specifically on L-band HH because of greater sensitivity to changes in Brigalow structure. Lower stature stands were associated with a greater contribution through direct ground scattering (Fig. 12a). As indicated in Fig. 12b, L-band HH σ° only increased above −22 dB at a height above 2 m, and trunk-ground double bounce scattering dominates this co-polarised channel increasing steadily above 2 m (Fig. 12b). Branch-ground scattering also increased, but less so within stands of higher density (Fig. 12c). Volume scattering (primarily from branches) showed a marked increase from stands exceeding 3.5 m in height (Fig. 12d). At L-band HV and for the taller stands, scattering was primarily from branch volume interactions and HV increases were relatively small and would only occur when stands support a more substantial crown layer.

Although the model may indicate a threshold for separating woody vegetation, this is different from that determined using the actual SAR data, with these differences attributable to instrument calibration errors and also errors in the modelling (e.g., in parameterisation and simulation). It should therefore be emphasized that the model corroborates the concept of using SAR for regrowth mapping whereas the actual thresholds ultimately need to be determined from the SAR data themselves.

7. Discussion

FPC has been extensively used in the classification of vegetation structure in Australia (Specht & Specht, 1999) and hence is an important discriminator of forest and non-forest vegetation. Using Landsat-derived FPC data alone, however, regrowth cannot be mapped with confidence as values rapidly increase to a level comparable with remnant mature forests. This increase in FPC is attributed to a greater allocation of biomass to the crown components during the early stages of regeneration and the high density of crowns associated with multiple stems, particularly in coppiced stands. For this reason, regrowth stands are classified as forest in the SLATS datasets and are not separated.

For the same reasons, regrowth cannot be distinguished from forest using C-band SAR data alone, whether obtained by airborne or spaceborne sensors. At C-band, microwaves interact primarily with the leaves and small branches of woody vegetation (Lucas et al., 2004) and hence C-band σ° provides a similar measure as FPC, as indicated by the close correspondence observed between these data at Injune, particularly at HV polarisations. The simulations based on the model of Durden et al. (1989) also indicated a rapid increase in C-band HV backscatter with stem height and density, which can be attributed to depolarisation of the microwaves by leaves and small branches and hence increases in volume scattering with canopy cover. As much of the herbaceous vegetation in the study region, and also throughout Queensland, is relatively dry throughout much of the year, minimal confusion with perennial woody vegetation occurs using either measure.

Using L-band and P-band data of all polarisations, and depending upon the size class distributions of woody stems and branches, the opposite occurs in that regrowth cannot be distinguished from non-forest areas, particularly in the earlier stages of growth or where growth is limited by environmental conditions. This was particularly evident when comparing the C-band, L-band and P-band image data themselves (Fig. 7), and also in the empirical relationships established between FPC and SAR σ° (Fig. 6). Through simulation modelling, the low value of σ° from the Brigalow regrowth was attributed to the lack of interaction between the ground and stem/branches, because of their small size in relation to that of the wavelength. This is illustrated diagrammatically, and for stems, in Fig. 13 where in the early stages of growth, scattering from the ground surface at the lower frequencies is typically specular and away from the sensor. However, with increases in stem size by a few

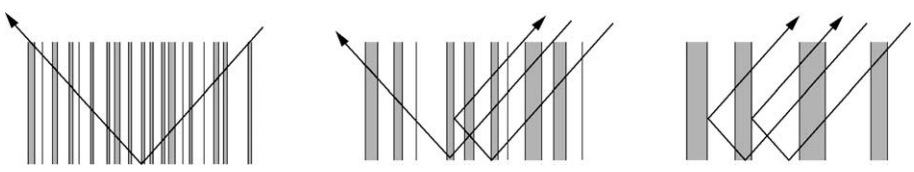

Fig. 13. Diagrammatic representation of the scattering process from Brigalow regrowth with increases in tree size.

individuals or the cohort as whole, stem-ground double bounce interactions become more dominant, which raises the level of σ° recorded, particularly at HH polarisations. Similarly, branch-ground interactions and also volume scattering increase (particularly at HV polarisations) with branch size. At L-band and P-band, and for the simulated stand, the transfer from specular to double bounce interactions (primarily with stems) occurs when stems are about 2 m and ~4–5 m in height, respectively. Simulations of L-band HV suggest also that interactions with branches only take place within stands exceeding 3.5–5 m.

Although regrowth cannot be discriminated using either of these data alone, mapping can be achieved using a combination of either FPC or C-band σ° and lower frequency L-band or P-band σ°. Specifically, all areas with an FPC above a threshold of 12% are mapped as forest and, within this category, all areas with an L-band or P-band σ° below a specified threshold (approximating to non-forest) are mapped as regrowth. Those remaining are classified as remnant forest.

Not all regrowth communities can be mapped using this approach. For example, older regrowth dominated by *E. mitchelli* and other *Acacia* and *Eucalyptus* species (including some stands of *A. harpophylla*) allocate a greater proportion of biomass to the trunks and are also generally single-stemmed, although multiple stems (rarely more than 4–5) may occur (Fig. 1b). These stands may support a basal area that is equivalent to that of similarly aged Brigalow regrowth, but the greater size of stems leads to a L-band or P-band σ° that is typically above that of non-forest areas. Areas of heath vegetation or understorey that typically support a large number of small stems with low basal area and high FPC may also be confused. Nevertheless, Brigalow-type regrowth is common throughout the region, particularly on cleared agricultural land, and hence the ability to map these areas represents a significant advance in Statewide forest assessment.

For regional mapping of Brigalow-type regrowth, the integration of Landsat-derived FPC and L-band HH and HV data provided by the ALOS PALSAR is advocated for several reasons. First, data from this sensor will be used to provide regional image mosaics of Australia (including Queensland) on at least an annual basis (Rosenqvist et al., 2004), which can be used in conjunction with the FPC datasets produced routinely by the SLATS programme. Second, by integrating these single-period PALSAR mosaics with the FPC data, classifications can be obtained by applying simple thresholds, thereby negating the need for extensive analysis of time-series datasets. Although close timing of the SAR and optical data acquisitions is preferable, the dates for which the FPC surfaces are generated are unlikely to influence the reliability of the regrowth maps, as the foliage cover is relatively constant, although it is affected by differences in photosynthetic activity of the herbaceous layer. The quantity and structure of woody material also remains relatively constant over an annual cycle (Grigg & Mulligan, 1999) and even between years, unless clearing events or adverse environmental conditions (e.g., drought, fire) occur. Although the use of FPC renders C-band SAR from spaceborne sensors effectively redundant for regrowth mapping, these data could nevertheless provide a viable alternative should the provision of Landsat sensor data discontinue.

The method for mapping regrowth has been developed using data acquired over forests associated with savanna–woodland formations and is only successful because of the relatively low rate of forest recovery and the openness of the canopy. The regression model used to derive a measure of horizontal vegetation structure (FPC) is preferred to spectral indices such as the Normalised Difference Vegetation Index (NDVI), because of its greater sensitivity to the complex spatial variation in soil colour existing in Queensland (Danaher et al., 2004). However, within the Injune study area, substituting NDVI might produce similar results as the predominantly sandy soils are bright and thus exhibit a strong spectral contrast with the photosynthetic canopy components. Of equal importance is that FPC is a measure of horizontal cover and as a result it does not change with the vertical growth of foliage shoots. Consequently, this measure shows less variation in response to changes in soil moisture and nutrients than one related to productivity (e.g., LAI or NDVI).

The FPC relationship was established for a wide range of forest types in Queensland, which are also typical to large areas of Australia. The approach of integrating FPC and L-band backscatter is therefore potentially applicable also to the Australian continent and also overseas (e.g., the Cerrado of Brazil and Acacia woodlands in southern Africa). However, results will be less reliable in the higher biomass forests of temperate or tropical regions where a closed canopy is typically formed within 5 years of growth (Lucas et al., 2000, 2002), often resulting in saturation of both vegetation indices and L-band backscatter due to the rapid accumulation of foliage cover and biomass.

8. Summary and conclusions

The research presented in this paper has proposed a simple method for mapping woody regrowth through integration of low frequency SAR data, acquired by both airborne or spaceborne platforms, and Landsat sensor-derived FPC. Evidence has been presented to support the method. In particular:

- Empirical relationships established between FPC and SAR σ° indicated increases in C-band σ° with FPC for all forest types but highlighted a lag in L-band and P-band σ°.
- Areas corresponding to Brigalow regrowth were observed within AIRSAR C-band data but these progressively disappeared within L- and P-band images.
- Simulation of SAR σ° from Brigalow stands of increasing height and density indicated a rapid increase in C-band HV but delayed response at the lower frequencies. At L-band and at HH polarisations, increases in σ° were associated primarily with trunk-ground scattering for stands greater than ~2 m in height and an associated reduction in ground scattering. Branch (volume) scattering became significant at heights exceeding 3.5–5 m and only where branches were of sufficient size to evoke a response. Lower returns were

observed at both L-band HV and P-band HH and HV polarisations.

Using simple thresholds of L-band HH σ° for areas mapped as forest based on a 12% FPC threshold, maps of woody regrowth were generated using both AIRSAR (for 2000) and also JERS-1 SAR data (acquired on four separate dates in 1994 and 1995). The mapped areas corresponded closely with those observed within hyperspectral data, time-series classifications of land cover change, and stereo aerial photography acquired in the different years. The areas of regrowth mapped using Landsat-derived FPC from 1995 and JER-1 SAR data from 1994–1995 were similar to those identified within true colour aerial photography and classified using the 2000 AIRSAR and FPC data. The analysis therefore supports the use of L-band data for mapping woody regrowth across the study area but also regionally.

A particular advantage of the method for mapping is that historical data layers are generally not required and relatively consistent estimates can be obtained from images acquired on different dates. The study therefore has implications for the assessment/characterisation, mapping and monitoring of re-growth within Queensland but potentially in other parts of Australia or overseas. Application of the method is likely to assist regional land cover change monitoring, carbon account-ing, sustainable utilisation of forests and the restoration of cover and biodiversity.

Following the launch of the ALOS PALSAR, dual polarimetric L-band HH and HV data from this sensor will be acquired twice annually over Queensland and processed into wall-to-wall image mosaics. By combining these data with FPC estimates generated over the same time-period, opportu-nities for mapping woody regrowth across the State will be provided. Integration of historical JERS-1 SAR data with proximal-date FPC rasters for the State might also allow regional mapping of regrowth for the early to mid 1990s, and the production of the Australia-wide JERS-1 SAR mosaic by JAXA is timely for this purpose. By comparing the two datasets, significant changes in land cover could be better quantified and existing classifications improved or validated. This study forms the basis for undertaking such mapping and monitoring.

Acknowledgements

The authors thank the Australian Research Council (ARC) under their SPIRT Program (for a grant to the University of New South Wales), the Queensland Department of Natural Resources and Mines (QDNR and M), Bureau of Rural Sciences (BRS), the Australian Greenhouse Office and the Cooperative Research Centre (CRC) for Greenhouse Accounting for collectively funding this research, the Queensland Department of Primary Industries (QDPI) Tropical Beef Centre and QDPI for assisting with destructive harvesting and the NASA Jet Propulsion Laboratory for acquiring the AIRSAR data. Definiens Imaging, particularly Ursula Benz, and the AMPER network are thanked for their support. Ake Rosenqvist and the Japan Space Exploration Agency (JAXA) are thanked for providing the JERS-1 SAR data. The anonymous reviewers are also thanked for their valuable comments on the manuscript.

References

ACF. (2002, June). Australian Conservation Foundation “Licking the salt”. *Natural advantage: A blueprint for sustainable Australia*. URL: http://www.acfonline.org.au

AGO. (2002). *National greenhouse gas inventory 2000-Land use change and forestry: 2000 Inventory and trends*. http://www.greenhouse.gov.au/inventory/2000/facts/pubs/05.pdf

AGO. (2005). *National greenhouse gas inventory 2000—Land use change and forestry: 2003*. http://www.greenhouse.gov.au/inventory/2003/index.html

Back, P. V., Burrows, W. H., & Hoffman, M. B. (1999). TRAPS: A method for monitoring the dynamics of trees and shrubs in rangelands. In D. Eldridge, & D. Freudenberger (Eds.), *People and rangelands: Building the future. Proceedings of the Sixth International Rangeland Congress, Townsville, Queensland, Australia* (pp. 742–744).

Baskerville, G. L. (1972). Use of logarithmic regression in the estimation of plant biomass. *Canadian Journal of Forestry Research*, *2*, 49–53.

Bond, W. J., & Midgeley, G. F. (2000). A proposed CO2 controlled mechanism of woody plant invasion in grasslands and savannas. *Global Change Biology*, *6*, 865–869.

Bureau of Meteorology. (1996). URL: http://www.bom.gov.au (Accessed April 1996).

Bureau of Meteorology. (2004). URL: http://www.bom.gov.au (Accessed April 2004).

Burrows, W. H., Carter, J. O., Scanlan, J. C., & Anderson, E. R. (1990). Management of savannas for livestock production in north-east Australia: Contrasts across the tree-grass continuum. *Journal of Biogeography*, *17*, 503–512.

Burrows, W. H., Henry, B. K., Back, P. V., Hoffman, M. B., Tait, L. J., Anderson, E. R., et al. (2002). Growth and carbon stock change in eucalypt woodland stands in north-east Australia: Ecological and greenhouse sink implications. *Global Change Biology*, *8*, 769–784.

Burrows, W. H., Hoffman, M. B., Compton, J. F., Back, P. V., & Tait, L. J. (2000). Allometric relationships and community biomass estimates for some dominant eucalypts in central Queensland woodlands. *Australian Journal of Botany*, *48*, 707–714.

Ceulemans, R., McDonald, A. J. S., & Pereira, J. S. (1996). A comparison among Eucalypt, Poplar and Willow characteristics with particular reference to a coppice growth-modelling approach. *Biomass and Bioenergy*, *11*, 215–231.

Danaher, T. J. (2002). An empirical BRDF correction for Landsat TM and ETM+ imagery. *Proceedings of the 11th Australasian Remote Sensing and Photogrammetry Conference, Brisbane, Australia, September 2002.*

Danaher, T. J., Armston, J. D., & Collett, L. J. (2004). A regression approach to mapping woody foliage projective cover in Queensland with Landsat data. *International Geoscience and Remote Sensing Symposium (IGARSS), Anchorage, Alaska, September 2004.*

De Fries, R., Hansen, M., Steininger, M., Dubayah, R., Sohlberg, R., & Townshend, J. (1997). Subpixel forest cover in Central Africa from multisensor, multitemporal data. *Remote Sensing of Environment*, *60*, 228–246.

De Vries, C., Danaher, T. J., & Scarth, P. (2004). Calibration of multiple Landsat sensors based on pseudo-invariant target sites in western Queens-land, Australia. *Proceedings International Geoscience and Remote Sensing Symposium (IGARSS).*

Dilworth, J. R., & Bell, J. F. (1971). *Variable probability sampling—variable plot and P.* Corvalis: OSU Book Stores.

Durden, S. L., Van Zyl, J. J., & Zebker, H. A. (1989). Modelling and observation of radar polarization signature of forested areas. *IEEE Transactions on Geoscience and Remote Sensing*, *27*, 290–301.

Environment Australia. (2001). *Brigalow Regrowth and the Environment Protection and Biodiversity Conservation Act 1999*. http://www.deh.gov.au/biodiversity/threatened/information/factsheets/brigalownote.html

EPA. (2000). Environment Protection Agency, Queensland Government. *Retaining and managing remnant brigalow vegetation*. URL: http://www.epa.qld.gov.au/publications/p00846aa.pdf/Retaining_and_managing remnant_brigalow_vegetation.pdf

Fairfax, R. J., & Fensham, R. J. (2000). The effect of exotic pasture development on floristic diversity in central Queensland, Australia. *Biological Conservation*, *94*, 11–21.

Fensham, R. J., McCosker, J. C., & Cox, M. J. (1998). Estimating clearance of Acacia dominated ecosystems in central Queensland using land-system mapping data. *Australian Journal of Botany*, *46*, 305–319.

Fernandes, R., Fraser, R., Latifovic, R., Cihlar, J., Beaubien, J., & Du, Y. (2004). Approaches to fractional landcover and continuous field mapping: A comparative assessment over the BOREAS study region. *Remote Sensing of Environment*, *89*, 234–251.

Galloway, R. W. (1974). Part1 Introduction, Lands of the Balonne-Maranoa Area, Part 7 Soils of the Balonne-Maranoa Area. *In CSIRO Division of Landuse Research, Land Research Series No. 34. Lands of the Balonne-Maranoa Area, Queensland*.

Grigg, A. H., & Mulligan, D. R. (1999). Litterfall from two eucalypt woodlands in central Queensland. *Australian Journal of Ecology*, *24*, 662–664.

Harrington, G. (1979). Estimation of above ground biomass of trees and shrubs in *Eucalyptus populnea* (F. Muell). Woodland by regression of mass on trunk diameter and plant height. *Australian Journal of Botany*, *2*, 135–143.

Harris, M. R., Lamb, D., & Erskine, P. D. (2003). An investigation into the possible inhibitory effects of white cypress pine (*Callitris glaucophylla*) litter on the germination and growth of associated ground cover species. *Australian Journal of Botany*, *51*, 93–102.

Hassett, R. L., Wood, H. L., Carter, J. O., & Danaher, T. J. (2000). A field method for statewide ground-truthing of a spatial pasture growth model. *Australian Journal of Experimental Agriculture*, *40*, 1069–1079.

Henry, B. K., Danaher, T., McKeon, G. M., & Burrows, W. H. (2002). A review of the potential role of greenhouse gas abatement in native vegetation management in Queensland rangelands. *Rangeland Journal*, *24*, 112–132.

Jeffrey, S. J., Carter, J. O., Moodie, K. B., & Beswick, A. R. (2001). Using spatial interpolation to construct a comprehensive archive of Australian climate data. *Environmental Modelling and Software*, *16*, 309–330.

Johnson, R. W. (1964). *Ecology and control of Brigalow in Queensland*. Brisbane: Department of Primary Industry.

Jones, K. L. (2000). Aerial photography interpretation for the Injune remote sensing sampling strategy. *Forest Ecosystem Research and Assessment Technical Report No. 00129*. Queensland Department of Natural Resources, Brisbane.

Kuhnell, C., Goulevitch, B., Danaher, T., & Harris, D. (1998). Mapping woody vegetation cover over the State of Queensland using Landsat TM. *9th Australasian Remote Sensing and Photogrammetry Conference.*

Liang, P., Moghaddam, M., Pierce, L., & Lucas, R. M. (2005). Radar backscatter model for multi-layer mixed species forests. *IEEE Transactions on Geoscience and Remote Sensing*, *43*(11), 2612–2626.

Lucas, R. M., Cronin, N., Lee, A., Witte, C., & Moghaddam, M. (2005). Empirical relationships between AIRSAR backscatter and forest biomass, Queensland, Australia. *Remote Sensing of Environment*, *100*, 407–425. doi:10.1016/j.rse.2005.10.019.

Lucas, R. M., Honzak, M., Curran, P. J., Foody, G. M., Milne, R., Brown, T., et al. (2000). Mapping the regional extent of tropical forest regeneration stages in the Brazilian Legal Amazon using NOAA AVHRR data. *International Journal of Remote Sensing*, *21*, 2855–2881.

Lucas, R. M., Moghaddam, M., & Cronin, N. (2004). Microwave scattering from mixed species forests, Queensland, Australia. *IEEE Transactions on Geoscience and Remote Sensing*, *42*, 2142–2159.

Lucas, R. M., Xiao, X., Hagen, S., & Frolking, S. (2002). Evaluating TERRA-1 MODIS data for discrimination of tropical secondary forest regeneration stages in the Brazilian Legal Amazon. *Geophysical Research Letters*, *29*, 42–51.

McDonald, R. C., Isbell, R. F., Speight, J. G., Walker, J., & Hopkins, M. S. (1990). Australian soil and land survey field handbook (2nd ed.). Melbourne: Inkata Press. 198 pp.

NASA National Aeronautical and Space Administration. (2004). *Landsat 7 Science data users handbook*. http://ltpwww.gsfc.nasa.gov/IAS/handbook/handbook_toc.html

Neldner, V. J. (1984). Vegetation survey of Queensland. South Central Queensland. *Queensland Botany Bulletin*, *vol. 3*. Queensland: Department of Primary Industries.

National Forest Inventory (NFI) (1998). Australia's State of the Forests, Report 1998. Canberra: Bureau of Rural Sciences.

National Forest Inventory. (2003). Forests at a glance. Canberra. http://www.affa.gov.au/corporate_docs/publications/pdf/rural_science/nfi/ataglance.pdf

NGGI. (1997). Carbon Dioxide from the Biosphere. *National greenhouse gas inventory, workbook 4.2*. Canberra: Environment Australia.

NLWRA National Land and Water Resources Audit. (2002). Australian terrestrial biodiversity assessment 2002. http://audit.ea.gov.au/ANRA/vegetation/docs/biodiversity/bio_assess_contents.cfm

QLD DPI. (1984). Queensland Department of Primary Industry (1984). *The Brigalow belt of Australia*. Brisbane: Royal Society of Queensland.

Rosenqvist, A., Milne, A. K., Lucas, R. M., Imhoff, M., & Dobson, C. (2003). A review of remote sensing technology in support of the Kyoto Protocol. *Environmental Science and Policy*, *6*, 441–455.

Rosenqvist, A., Shimada, M., Watanabe, M., Tadono, T., & Yamauchi, K. (2004). Implementation of Systematic Data Observation Strategies for ALOS PALSAR, PRISM and AVNIR-2. *Proc. of the International Geoscience and Remote Sensing Symposium (IGARSS'04). Anchorage, USA, Sept. 20–24, 2004*.

Salvador, R., & Pons, X. (1998). On the reliability of Landsat TM for estimating forest variables by regression techniques: A methodological analysis. *IEEE Transactions on Geoscience and Remote Sensing*, *36*(6), 1888–1897.

Scanlan, J. C. (1991). Woody overstorey and herbaceous understorey biomass in *Acacia harpophylla* (brigalow) woodlands. *Australian Journal of Ecology*, *16*, 521–529.

SLATS. (1999). *The Statewide Landcover and Trees Study (SLATS)*, Queensland Department of Natural Resources and Mines. URL: http://www.nrm.qld.gov.au/slats/pdf/paste9597-11.PDF

SLATS. (2003). *The Statewide Landcover and Trees Study (SLATS)*, Queensland Department of Natural Resources and Mines. URL: http://www.nrm.qld.gov.au/slats/pdf/slats9901.pdf

Smith, D. M., Shields, P. G., & Danaher, T. J. (1994). An Assessment of the Extent of Clearing in South-central Queensland. *Land resources bulletin*. Queensland: Department of Primary Industries.

Specht, R. L., & Specht, A. (1999). Australian plant communities: Dynamics of structure. *Growth and biodiversity.* Oxford University Press.

Van Zyl, J. J., Zebker, H. A., & Elachi, C. (1987). Imaging radar polarisation signatures. Theory and observation. *Radio Science*, *22*, 529–543.

Walthall, G. L., Norman, J. M., Welles, J. M., Campbell, G., & Blad, B. L. (1985). Simple equation to approximate the bi-directional reflectance from vegetative canopies and bare soil surfaces. *Applied Optics*, *24*(3), 383–387.

Zebker, H. A., Van Zyl, J. J., & Held, D. N. (1987). Imaging radar polarimetry from wave synthesis. *Journal of Geophysical Research*, *92*, 683–701.